Experience in Communication & Radar

1. **VHF Antenna Observation of Solar Radio Bursts**: 2023/12 ~ 2024/06

In the first half of 2024, I collaborated with Professor Yang and junior student Mr. Huang from our department on a project involving the observation of **solar radio bursts** using a **Very High Frequency** (VHF) antenna. The primary goal was to qualify our observation station at National Central University for participation in the e-Callisto program (International Network of Solar Radio Spectrometers). The observation focused on **transient phenomena** in the **solar corona**. We utilized an antenna system installed by previous students, with signals amplified through a Low Noise Amplifier (LNA) and transmitted to a computer via a receiver for further analysis.

I assisted the professor in refining the observational data, measuring key parameters of the antenna system, and establishing the specifications for the observation station at National Central University. During the data processing phase, I applied radar signal analysis techniques and successfully identified signal enhancements within specific frequency bands over short durations in the spectrogram. By cross-referencing data from other international observation stations, we confirmed that Taiwan possesses the capability to detect solar radio bursts. This experience deepened my understanding of radio observation and signal processing, while also strengthening my practical skills in radar signal analysis.

Figure1: Professor Yang's team and the director of the Zhongli VHF Radar Station took a group photo in front of the observation antenna.

2. **Radar Project-Target Signal Analysis**: 2022/09 ~ 2023/02

(1) Radar Parameters:

- Pulse Width (τ): 2 μs
- Radar Antenna Transmission Frequency: 52 MHz
- Inter-pulse period (IPP): 200 μs
- Duty Cycle (τ/ IPP): 1% (Acceptable if <7.5%)
- Minimum Sampling Distance: 2 km
- Receive Delay Time (Delay time): $\frac{2000\times2}{C}$ = 13.333μs (related to the minimum sampling distance; C is the speed of light)
- Maximum sampling distance: 28.1 km
- In-phase integration count: (Coherent Integration, CI): 256
- Time resolution (Δt): IPP * CI = 0.0512 seconds
- Spatial resolution (ΔR): τ * C / 2 = 300 m
- Number of range gates: 87 (However, the data from the firstGateis meaningless)
- Total time (T): 60s
- Number of data points per gate: T / Δt = 1171
- Cutoff Frequency (Nyquist Frequency): $\frac{1}{2\times\Delta t}$ = 9.766 Hz
- Frequency Resolution (Δf): 1 / (1024 * Δt) = 0.01909 Hz
- Peak Transmit Power: 40 kW
- ST Array Antenna Pointing Settings:

Channel 1	Channel 2	Channel 3
Tilt	Vertical (Receive only)	Vertical
West	Verticle	Verticle
North	Verticle	Verticle
East	Verticle	Verticle
South	Verticle	Verticle

(2) Time-Domain Analysis of In-Phase (I) and Quadrature (Q) Signal Components：

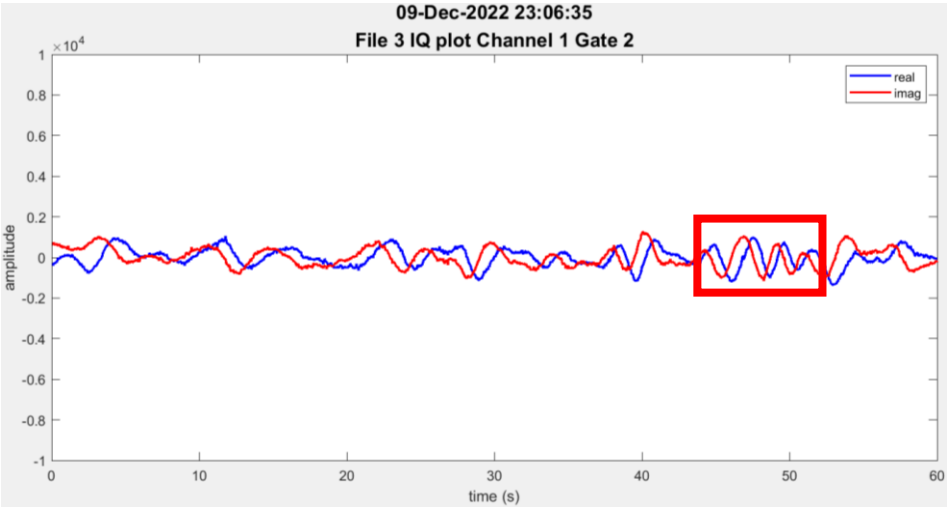

Figure 2: Time Series of In-Phase (I) and Quadrature (Q) Signals – File 3.

Explanation: When the original radar signal (assumed to be a cosine function) enters the mixer, it is split into two paths—one multiplied by a cosine wave and the other by a sine wave. Using the trigonometric product-to-sum identities, this results in components corresponding to a cosine and a negative sine signal. The in-phase (I) component can thus be interpreted as the cosine function, while the quadrature (Q) component corresponds to the negative sine function. As shown in the red box of Figure 2, the phase difference between Q and I is –90°.

(3) IQ Constellation Diagram and Gaussian Distribution：

The purpose of shifting the IQ components is to eliminate the interference caused by delay time, thereby improving the quality of subsequent spectral analysis. **Delay time** refers to the time difference between the transmitted signal and the first received echo. If this time interval is too short, the received echo may be affected by the strong transmitted signal, resulting in degraded echo quality. When setting the minimum sampling range, the effect of delay time must be taken into account. In this case, the minimum sampling range should be greater than 1.5 km (corresponding to 10 μs).

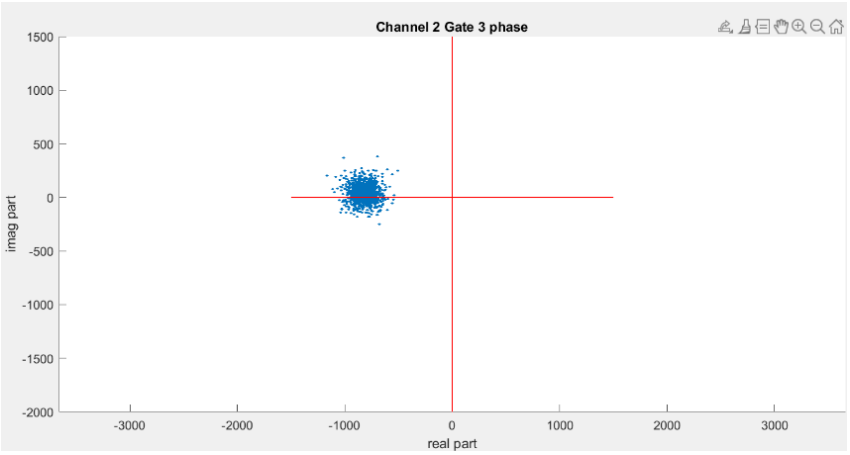

Figure 3: IQ Scatter Plot Before Shifting.

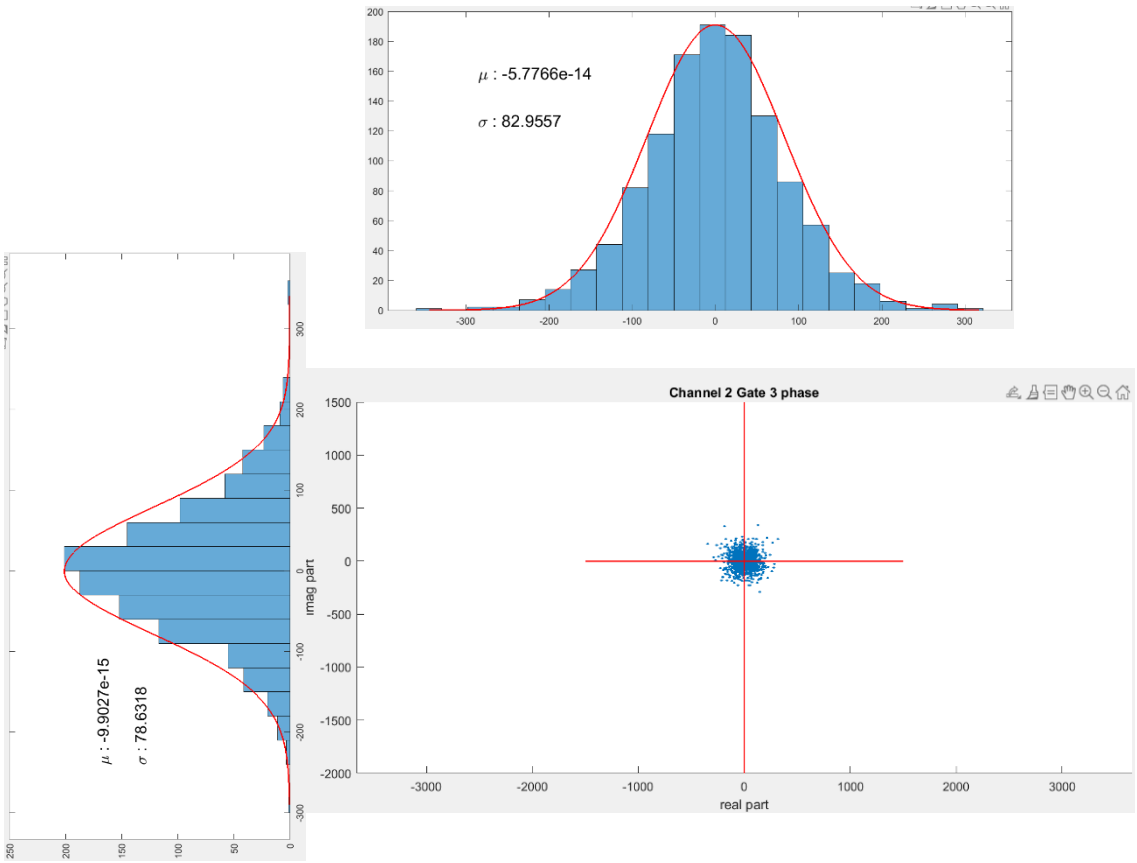

Figure 4: Shifted IQ Scatter Plot and Gaussian Distribution

Explanation: It can be observed that, after shifting, the IQ components exhibit a Gaussian distribution. This indicates high-quality echo data, which is a desirable condition for radar signal analysis.

(4) RTI (Range-Time-Intensity):

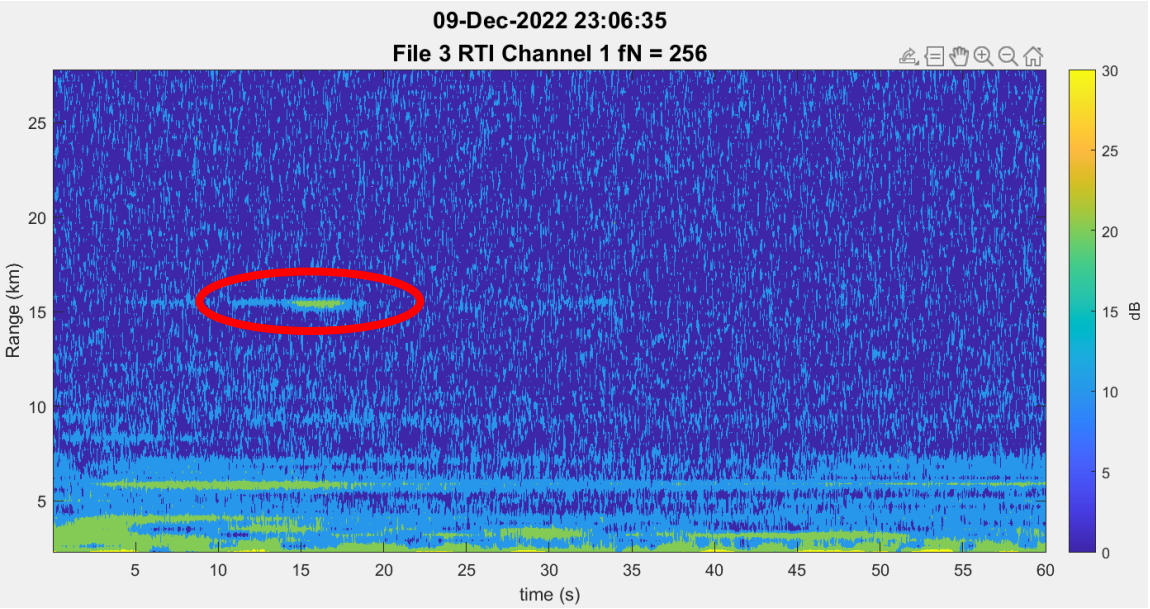

Figure 5: Radar echoes received when the antenna was tilted westward, covering an observation range from 2.3 to 28.1 km.

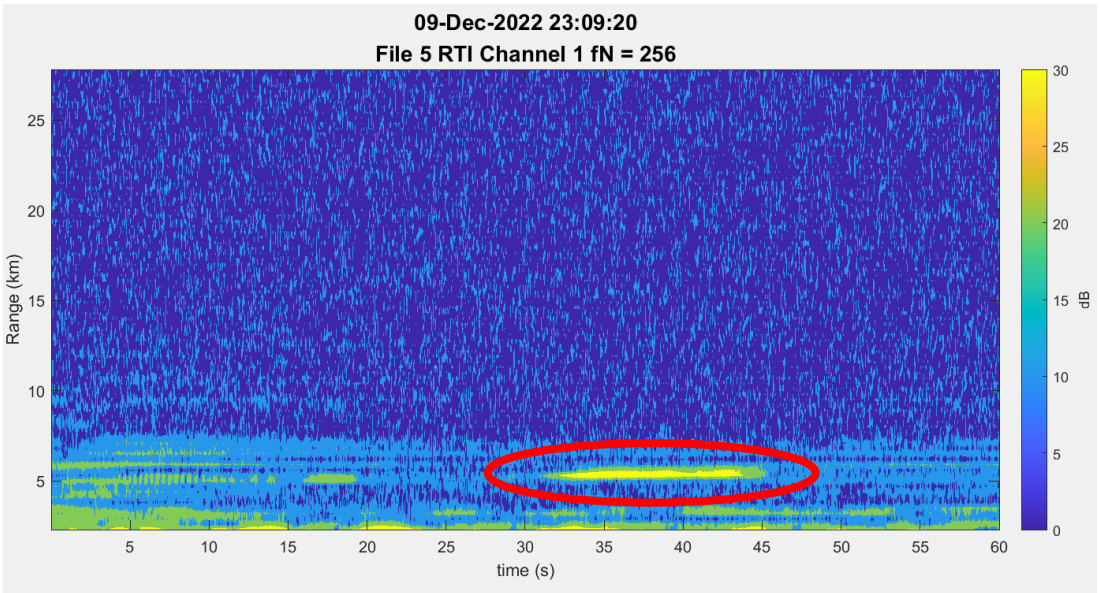

Figure 6: Radar echoes received when the antenna was pointed vertically toward the sky, covering an observation range from 2.3 to 28.1 km.

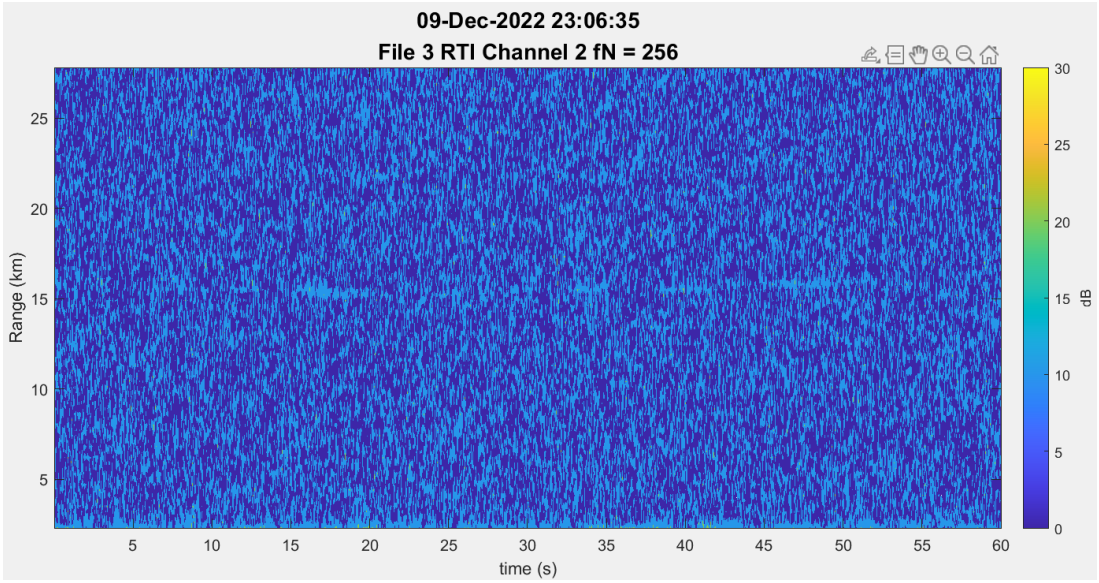

Figure7: Radar echoes received when the antenna was tilted eastward, covering an observation range from 2.3 to 28.1 km.

Explanation: Figure 5 shows echoes received by the ST array antenna, tilted westward, on December 9, 2022, at 23:06:35. The echo strength (in dB) is calculated using the formula:

$$dB = 20 \times \log_{10}\left(\frac{A_1}{A_0}\right)$$

where $A_1 = \sqrt{I^2 + Q^2}$, and A_0 represents the noise level (the average amplitude of the smallest 30% of different gates, sorted in increasing order). Since Channel 1 is tilted, the 15 km mark in Figure 5 does not correspond to the actual height. The area circled in red likely represents echoes caused by an aircraft. If the echoes were caused by rain, the range gate would have a larger span. Figure 6 represents data from Channel 2, where the antenna is oriented vertically. The received echo power is usually much lower in this case. Figure 7, like Figure 5, also shows echoes caused by an aircraft.

(5) Spectral Analysis: Without Non-In-Phase Integration vs. Non-In-Phase Integration:

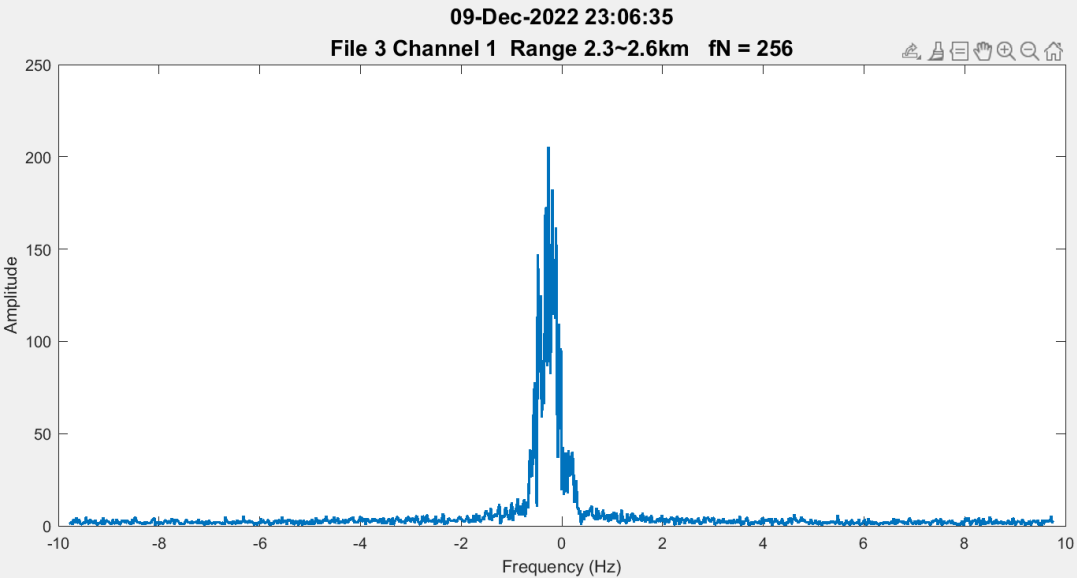

Figure 8. Spectrum Without Non-In-Phase Integration.

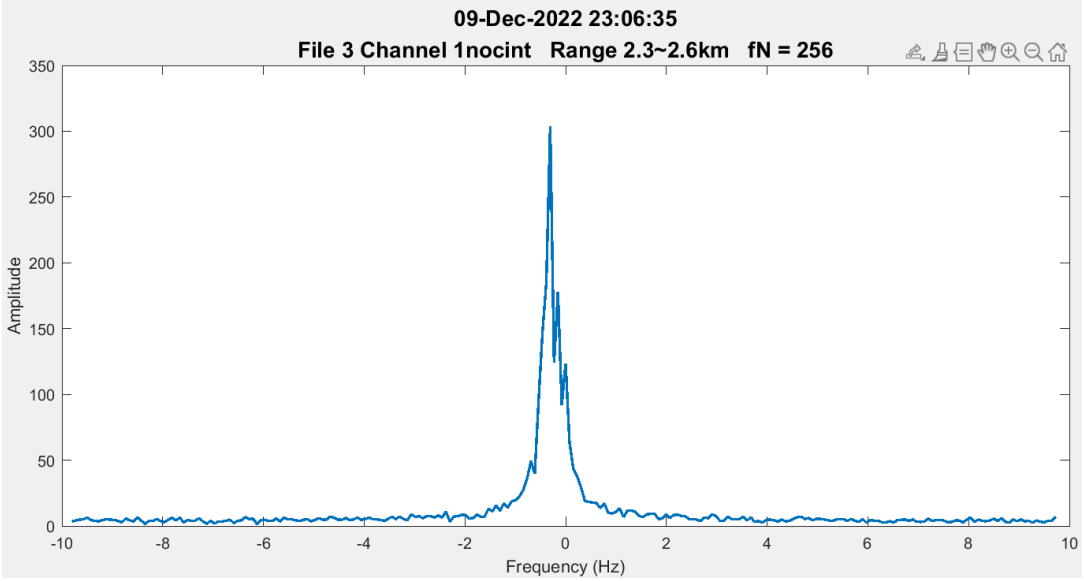

Figure 9: Spectrum with Non-In-Phase Integration.

Explanation: Non-in-phase integration involves modifying the original radar signal, which is processed with a 1024-point FFT, by dividing the signal into four equal parts. Each segment is then processed with a 256-point FFT. The results are summed and divided by four. This division by four is necessary because a 1024-point FFT is scaled by 1/1024, while a 256-point FFT is only scaled by 1/256, so the factor of four compensates for this difference. The purpose of non-in-phase integration is to smooth the original radar spectrum, reducing interference during subsequent data

analysis.

(6) Spectrum: Without Non-In-Phase Integration vs. Non-In-Phase Integration:

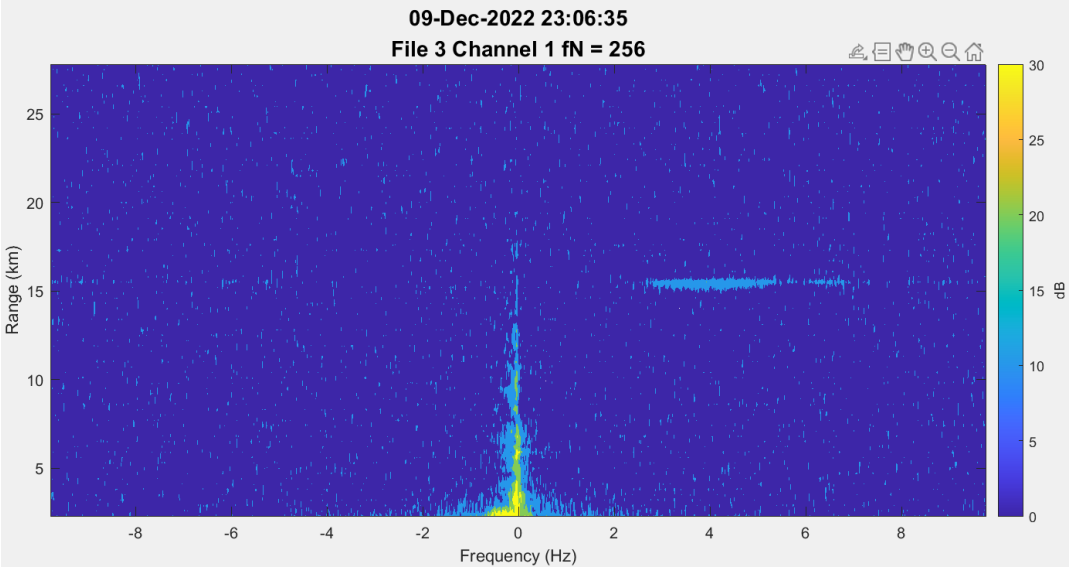

Figure 10: Radar spectrum processed without applying non-in-phase integration

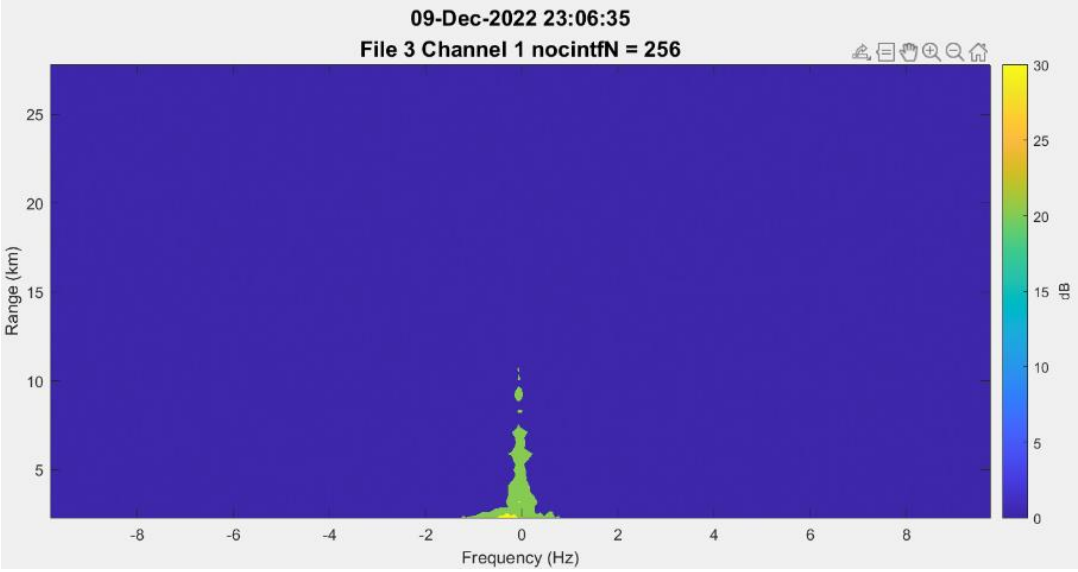

Figure 11: Radar Spectrum after Non-In-Phase Integration.

The FFT results from each range gate are aggregated to produce a full-range radar spectrum. While the overall difference between the non-integrated and non-in-phase integrated spectra is minimal, the latter shows significantly reduced visible noise, suggesting effective spectral smoothing.

(7) Elimination of White Noise：

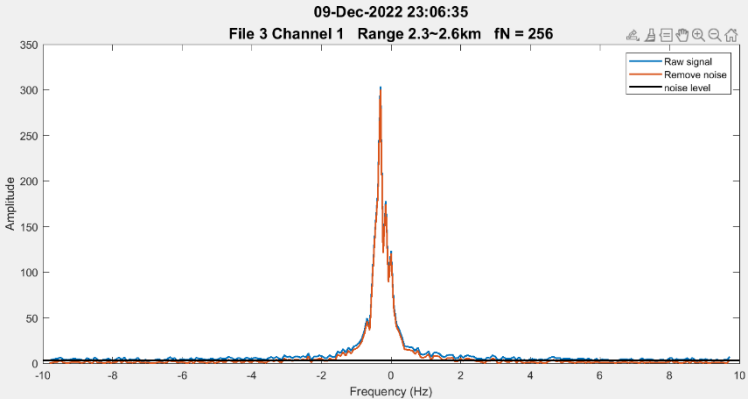

Figure 12: Spectrum Comparison: Before vs. After White Noise Removal.

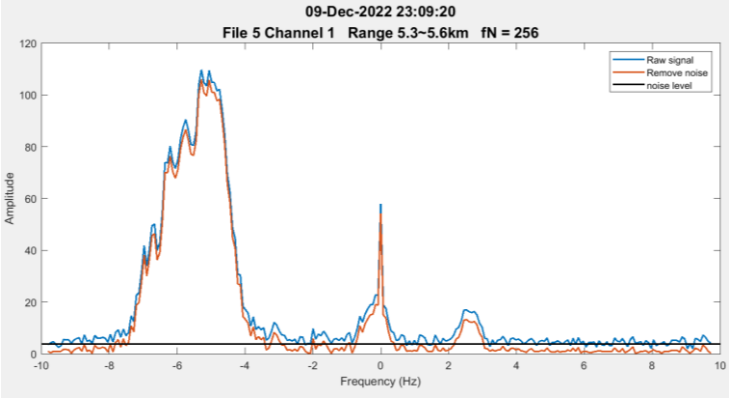

Figure 13: Spectrum Comparison: Before vs. After White Noise Removal (Clear Signal Present).

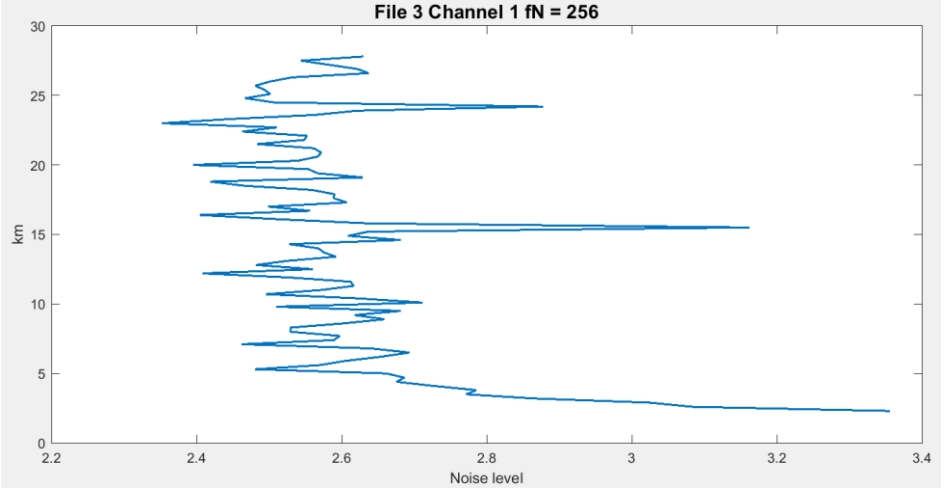

Figure 14. Variation in Noise Level as a Function of Range.

Explanation: Each gate has a different noise level. As in the previous method, the average of the lowest 30% of the signal amplitudes is used to estimate the noise level. After subtraction, any resulting power values less than zero are set to zero. White noise appears across all frequency bands and is generally caused by random variables. As shown in Figure 14, the noise is more

significant at distances less than 5 km, likely due to stronger interference near the ground, such as moisture, power lines, and aircraft. Additionally, radar echoes at around 15 km also show signs of aircraft interference.

(8) 3-Point Running Mean Comparison：

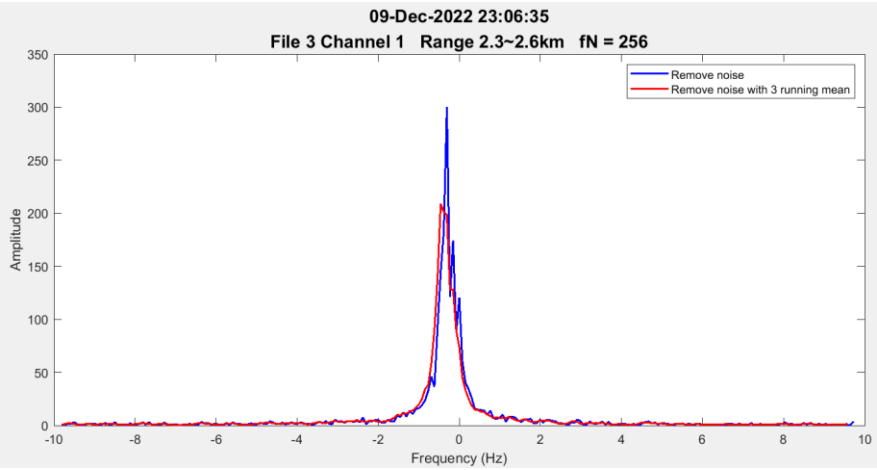

Figure 15: The signal, after white noise removal, is processed using a 3-point running mean.

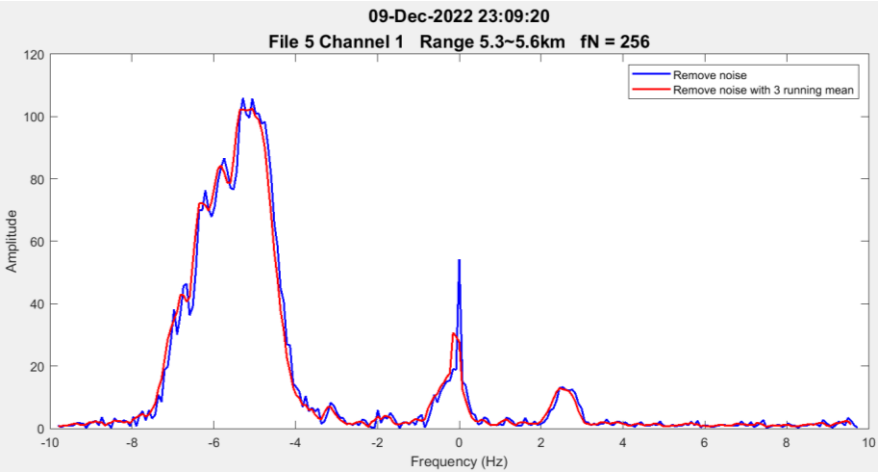

Figure 16: The signal, after white noise removal, is processed using a 3-point running mean.

Explanation: The original signal in Figure 15 shows a sudden spike in power at a certain frequency band. This is due to the signal being a random variable. To smooth out this power fluctuation, a running mean is applied.

(9) Gaussian Fit (Method of Moments):

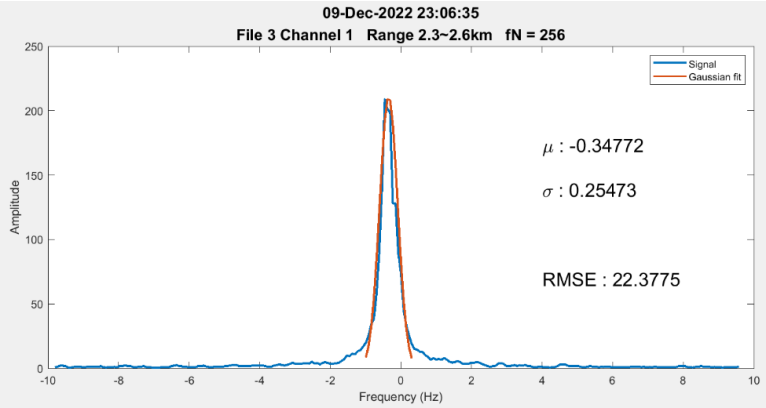

Figure 17. Gaussian Fit Applied to the Spectrum.

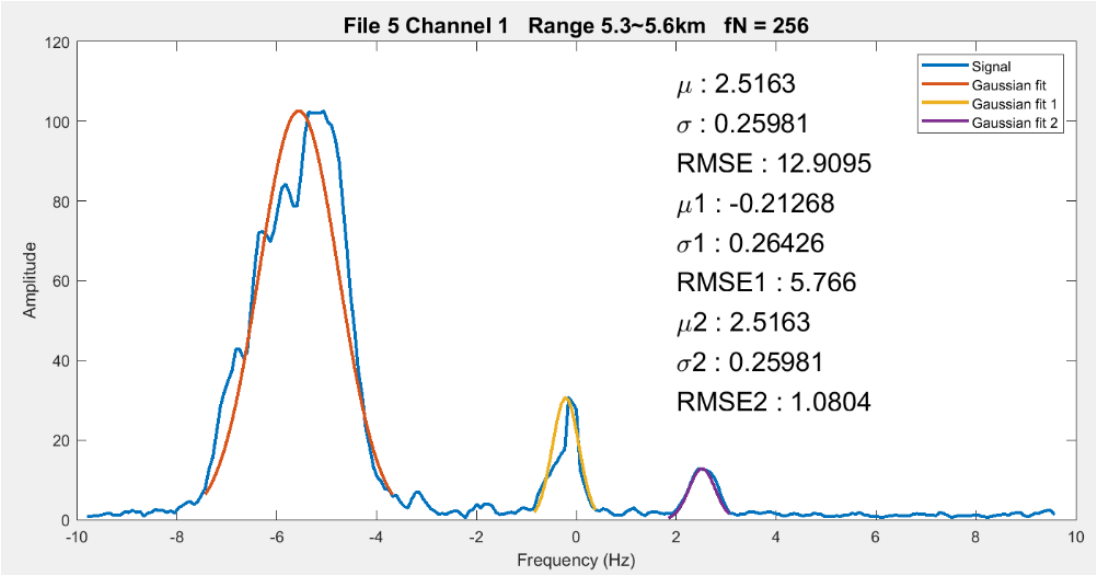

Figure 18. Gaussian Fit Applied to the Spectrum.

Explanation: The mean and standard deviation of the spectrum are calculated using the method of moments. The formulas are as follows:

- $m_0 = \int_{-\infty}^{\infty} y\,dx$
- $m_1 = \int_{-\infty}^{\infty} x \cdot y\,dx$
- $m_2 = \int_{-\infty}^{\infty} x^2 \cdot y\,dx$

The mean μ and standard deviation σ are given by:

- $\mu = \frac{m_1}{m_0}$

- $\sigma = \sqrt{\frac{m_2}{m_0} - \left(\frac{m_1}{m_0}\right)^2}$

The range of the x-axis is determined by the frequency corresponding to 10% of the maximum power in the spectrum, which is used as the interval for the Gaussian distribution. The Root Mean Square Error (RMSE) is then used to assess how well the Gaussian distribution fits the original spectrum. A smaller RMSE indicates a better fit.

(10) Spectrum of a Specific Event：

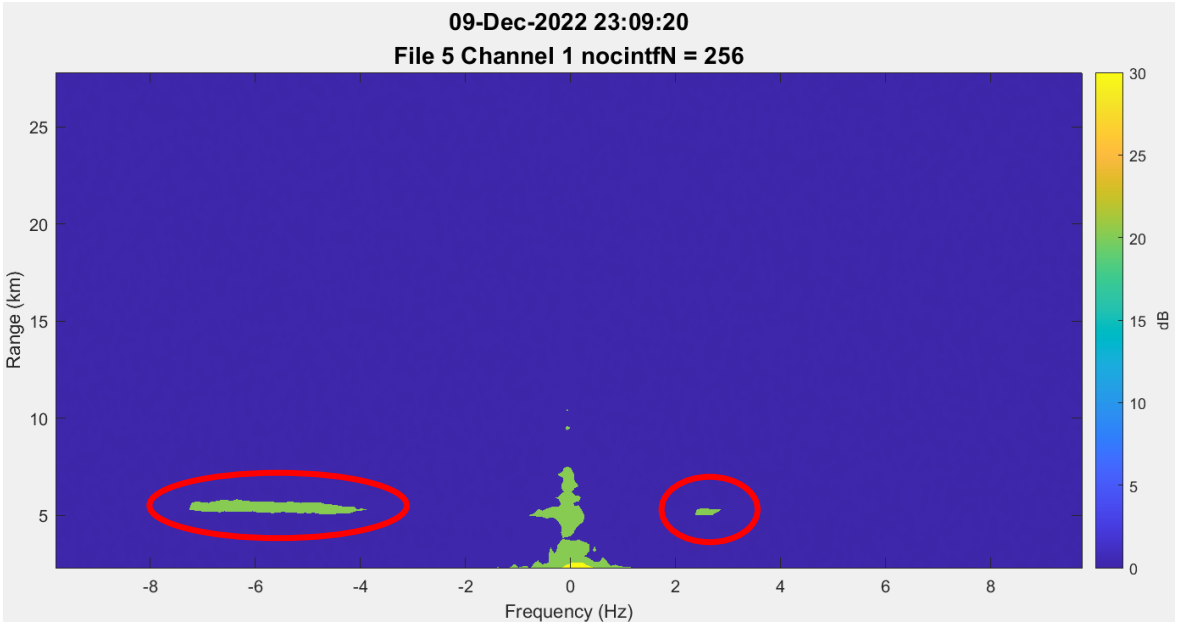

Figure 19. Spectrum After Non-In-Phase Integration Processing.

Explanation: From Figure 19, it can be observed that there is a stronger echo at approximately 6 km from the antenna, which is likely caused by an aircraft, as it coincides with the expected altitude. If the echo were due to rain, the range of the echo should be much broader in height, but Figure 19 exhibits this phenomenon. However, if the source were an aircraft, the echo frequency would be continuous. Interestingly, in Figure 19, there is a noticeable reduction in the echo at around -4 to 2 Hz. This is an intriguing observation, as the antenna consists of a main lobe and side lobes. The echo between the two lobes tends to be weaker, which is why the reduction in the echo is observed at frequencies where there are no lobes, explaining the drop in signal strength.

Project Reflection:

In this project, I gained a deep understanding of the radar station's structure. By using a Low Noise Amplifier (LNA), I was able to amplify the weak echo signals from the ionosphere array and ST array, improving the quality of the signals for subsequent processing. I also utilized Fourier Transform and convolution to derive the mathematical formula for the Running Mean Filter with different equal weights, which helped improve the signal-to-noise ratio.

In terms of signal analysis, I observed that if the IQ component scatter plot deviates from the origin, it may indicate interference from the transmitting end. This requires further consideration of the Delay Time effect for calibration. The overall project covered the complete process from signal reception to processing, involving many technical details that are difficult to list exhaustively.

Through this project, I not only enhanced my practical skills in "radar signal analysis" but also laid a solid foundation for my future exploration in the field of "satellite communication."